Original Article
cnj.araku.ac.ir

☑ Cite This: Colloid Nanosci. J. 3(3) (2025) 669-681 DOI: 10.61882/CNJ.3.3.669

Fabrication of novel electrochemical sensor with CeO_2 nanoparticles for determination of dopamine in real samples

Masoud Rezaeinasab[1*], Mehdi Hatefi Ardakani[1], Roya Afsharipour[2]

[1] Department of Chemistry, Faculty of Science, Vali-e-Asr University of Rafsanjan, Rafsanjan, Iran
[2] Department of Chemistry, Faculty of Science, Yazd University, Yazd, Iran

ARTICLE INFO

Article History:
Received 2025-10-03
Revised 2025-12-13
Accepted 2025-12-16
Published 2025-12-24

Corresponding Authors:
Masoud Rezaeinasab
Email:
m.rezaeinasab@vru.ac.ir

ABSTRACT

The precise monitoring of dopamine, an essential neurotransmitter, requires efficient sensing strategies, and modified electrodes provide a promising route toward achieving this goal. In this study, a carbon paste electrode (CPE) modified with cerium oxide nanoparticles (CeO_2/CPE) was developed and employed for the determination of dopamine. The synthesized cerium oxide nanoparticles were characterized using Fourier-transform infrared spectroscopy (FT-IR), X-ray diffraction analysis (XRD), scanning electron microscopy (SEM), Raman and UV-visible spectroscopy. The structural properties (porosity and specific surface area) of nanoparticles were evaluated by Brunauer–Emmett–Teller (BET) analysis. Based on the obtained results from various characterizations, the synthesis of cerium oxide nanoparticles was successfully achieved. The obtained results from cyclic voltammetry (CV) indicate that the CeO_2/CPE, benefiting from the synergistic effects of the nanoparticles, enhances electron-transfer kinetics and exhibits pronounced electrocatalytic activity, thereby providing an effective platform for dopamine (Dop) analysis. According to the differential pulse voltammetry (DPV) results, the calibration curve for Dop was linear in the range of 0.5-80 µM under optimum conditions. The calculated detection limit was 0.17 µM. Analysis of the results reveal that the CeO_2/ CPE has great selectivity, reproducibility, stability, repeatability, and can be efficiently employed for the determination of Dop in blood serum samples.

KEYWORDS: *Sensor; Dopamine; CeO_2 nanoparticles; Modifier*

1. Introduction

Dopamine (Dop), as a neurotransmitter, can transmit the message from neurons to central neurons in mammals [1]. The high concentration of Dop into the normal levels causes a variety of serious health problems such as senile dementia, Parkinson's disease, high pressure, schizophrenia, etc [2-6]. Thus, the determination of Dop is vital to control the concentration of Dop in the mammalian body. Accordingly, the detection of Dop is interest to researchers using various assessment techniques such as spectrofluorimetric and HPLC [7-11]. These techniques face several drawbacks, including complex extraction procedures, sensitivity to temperature, high instrument costs, and limited sensitivity [12, 13]. To overcome these limitations, various electrochemical detection methods have been developed for the quantification of biochemical molecules, offering advantages such as high sensitivity, excellent selectivity, rapid response, and cost-effectiveness. Modified electrodes play a crucial role in electrochemical applications, enabling highly selective and accurate detection of analytes in environmental, medical, and biological systems [14-21]. Materials based on carbon, including graphite, glassy carbon, carbon nanotubes, and graphene, are frequently utilized to enhance electrode properties due to their superior conductivity and adaptability for surface functionalization. Modification of electrodes with carbon nanomaterials enhances their charge separation efficiency. Recently, different materials as modifiers have emerged regarding electrochemical sensing of the important biological species such

as Dop, ascorbic acid, uric acid, tryptophan, etc [22-25]. Our research investigations revealed that r-graphene oxide, graphene oxide, and metal oxide-rGO composites are widely applied for the electrochemical detection of DA. In addition to the mentioned compounds, other substances such as CuO-MgO, $LaFeO_3$, carbon quantum dots/copper oxide nanocomposite and Zn-Co_2O_4 have been used for modification of electrodes and measurement of dopamine [26-29].

To date, different polymers, metal oxide NPs (MO NPs), metal NPs, and various nanocomposites such as $CoFe_2O_4/SiO_2$, $Tb_2Ti_2O_7$, Bi_2O_3/MgO/Fe_2O_3, CoNi-MOF/RGO and Ni-MOF have been employed to modify the sensing layer of the working electrode for the measurement of different species [30-34]. The materials that are suggested for this purpose possess good properties such as low toxicity, high conductivity and high stability, great biocompatibility, and great electronic properties [35]. In recent years, metal oxides and their applications in various fields have attracted significant attention from researchers. Reliable electron conduction and quick response led to achieving proper access in the detection, biomedical applications, and catalysis regions [36-38].

Among various types of metal oxide NPs, cerium oxides (CeO_2) semiconductors with a band gap of 3.19 eV have been utilized for the detection of adenine, guanine [39], and uric acid in biological fluids [40], and nitrite [41]. CeO_2 is a great choice for use in biosensors due to its unique properties, such as chemical stability, biocompatibility and high electrocatalytic properties [42]. Considering the unique and special properties of nanoparticles, their application in electrode modification can lead to enhanced sensitivity and a lower detection limit for the measurement of various species using electrochemical methods. In the drug industry, drug analysis has an important role for public health because it can affect under effectiveness of drug quality and drug dosage in the human body, and thus, we designed a new method for Dop determination.

In the present study, a new carbon paste electrode modified with CeO_2 nanoparticles was constructed and applied for sensitive determination of Dop (Scheme 1). The capability of the newly designed Dop sensor based on CeO_2 nanoparticles was investigated by cyclic voltammetry and differential pulse voltammetry. Cerium oxide alone coated on the carbon paste electrode caused the oxidation current to increase and the potential to decrease, and can be used as an effective platform for dopamine oxidation and measurement. The designed sensor indicated good selectivity and reliable reproducibility for the Dop detection in real biological fluids. The proposed CeO_2/CPE sensor lies in its simple fabrication strategy, the ease of electrode modification, and its superior analytical performance compared with previously reported. In particular, the sensor exhibits a markedly lower detection limit, a wider linear range, and a straightforward carbon paste electrode modification process, all of which distinguish our approach from earlier designs.

2. Experimental

2.1 Chemical and Apparatus

CeO_2 nanoparticles were synthesized according to a previous literature [43]. Dopamine, graphite fine powder, and viscous paraffin were obtained from Merck Company and used as received. All the other chemicals were also purchased from Merck Company in analytical grade and were used without any further purification. FT-IR spectra were recorded in the 4000–400 cm^{-1} region, using KBr disks, on a Thermo SCIENTIFIC model NICOLET iS10 spectrophotometer. Power X-ray diffraction (XRD) was performed on a Philips X'pert diffractometer with Cu Kα (λ = 0.154 nm) radiation. The SEM was performed with a TESCAN instrument model VEGA3. The absorption spectra were obtained using an Analytic Jena SPECORD-205 spectrophotometer in the range of 190-1000 nm and at 1nm resolution. The electrochemical measurements were performed with an Autolab potentiostat/Galvanostat (PGSTAT-101). The experimental conditions were controlled using Nova 2.1 software installed on a PC computer. The working, counter, and reference electrodes were carbon paste electrodes modified with CeO_2 nanoparticles (CeO_2/CPE), a platinum electrode, and an Ag /AgCl (sat.), KCl (3 M) electrode, respectively. All potential in this research was reported with respect to this reference electrode. The Metrohm model 691 pH/mV meters were used for pH adjustments.

2.2 Synthesis of CeO_2 nanoparticles

The sol–gel method is a widely used approach for synthesizing CeO_2 nanoparticles due to its simplicity, cost-effectiveness, and ability to control

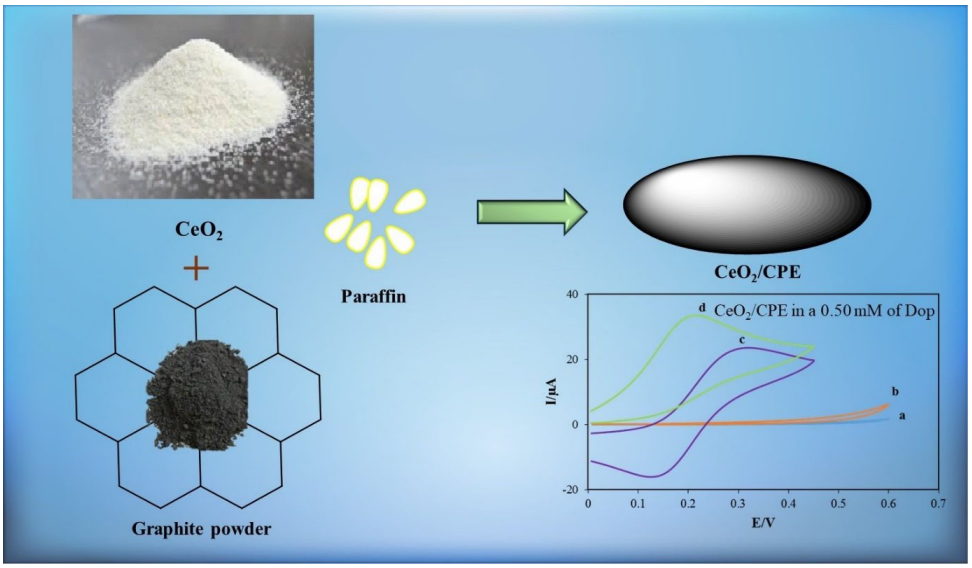

Scheme 1. Schematic representation of the designed CeO_2/CPE modified electrode.

particle size and morphology. In this process, a cerium precursor is dissolved in a suitable solvent to form a colloidal solution (sol). Hydrolysis and condensation reactions lead to the formation of a three-dimensional network (gel). The gel is then dried and calcinated at elevated temperatures to obtain crystalline CeO_2 nanoparticles. This method allows precise control over particle size, uniformity, and surface properties, making it highly suitable for catalytic and sensor applications. CeO_2 nanoparticles were prepared according to the previously reported procedure [43]. For this case, 4.0 g of ammonium cerium (IV) nitrate (10 mM) and 4.2 g of citric acid (20 mM) were dissolved in 50 mL of distilled water and stirred vigorously for 20 min. During stirring, ammonia solution was added dropwise, and the pH of the solution was increased to about 10. The solution obtained was heated on a hot plate under constant stirring. After a certain period, self-combustion takes place. The formed ash was collected in a crucible and then calcinated in the furnace at 300 °C for 3 h. The obtained product was a light-yellow powder.

2.3 Preparation CeO_2/CPE sensor

To prepare the CeO_2/CPE sensor, a mixture of graphite powder (0.46 g), CeO_2 nanoparticles (0.04 g), and ~20 μL of paraffin oil was blended by hand in a mortar and pestle. Then, it was inserted at the bottom of a glass tube (internal radius: 2 mm and 10 cm long). Electrical contact was made by pushing a conductive copper wire into the end of a glass tube, which stuck to the carbon paste (Scheme 1). It is necessary to have a fresh electrode surface. The new surface is generated by extruding a small plug of paste with a stainless-steel rod and smoothing the resulting surface on the white paper.

3. Results and Discussion

3.1 Characterization of CeO_2 nanoparticles

The FT-IR spectra of synthesized CeO_2-NPs are shown in Fig. 1 (A). The intense bands at 3423 and 1640 cm^{-1} are attributed to the ν(O–H) mode and δ(OH) of H_2O molecules that are linked to CeO_2-NPs, respectively [44]. The vibration at 521 cm^{-1} is considered a characteristic phonon mode for CeO_2-NPs [45]. The bands at 1050 and 1250 cm^{-1} are ascribed to the ν(Ce-O-Ce) vibration [46]. The band at 1383 cm^{-1} is indicative of the N=O stretching vibration that was produced by the trace amount of nitrate [47]. In summary, the synthesized CeO_2 nanoparticles were thoroughly characterized to evaluate their structural and textural properties. FT-IR analysis confirmed the formation of CeO_2 with characteristic Ce–O vibrations at 521 cm^{-1} and Ce–O–Ce network bands at 1050–1250 cm^{-1}. Raman spectroscopy was employed to investigate the structural of the synthesized CeO_2 nanoparticles. Fig. 1(B) represents the typical Raman-scattering spectrum of CeO_2 nanoparticles. A prominent sharp peak appeared in the Raman-scattering spectrum of the CeO_2 nanoparticle at

~ 459 cm^{-1} corresponding to the F_2g vibrational mode of cerium oxide nanoparticle. This mode is characteristic of the symmetric stretching of the O–Ce–O bonds in the lattice. No significant additional peaks were observed, indicating that the sample is phase-pure and free from secondary cerium oxide phases [48].

The X-ray diffraction analysis confirmed the formation of pure cerium oxide nanoparticles with was shown in Fig. 2. The diffraction pattern exhibited characteristic peaks corresponding to the (111), (200), (220), (311), (222), (400), (331), (420), and (422) crystallographic planes at 2θ values of approximately 28.6°, 33.2°, 47.6°, 56.4°, 59.2°, 69.5°, 76.8°, 79.2°, and 88.6°, respectively. The most intense peak at 2θ = 28.6° corresponds to the (111) plane, which is characteristic of the CeO_2 phase [49]. The average crystallite size (D) of the CeO_2 nanoparticles was calculated via the Scherrer equation ($D = 0.94\lambda/\beta\cos\theta$) where D is the average crystalline domain size perpendicular to the reflecting planes, λ is the x-ray wavelength, β is the full width at half maximum (FWHM) is in radians, and θ is the diffraction angle. The mean size of the particle was be calculated 9.2 nm. To further evaluate the crystallite size and lattice strain of the synthesized CeO_2 nanoparticles, the Williamson–Hall (W–H) models was employed. The W–H approach ($\beta\cos\theta=0.94\lambda/D+4\varepsilon\sin\theta$, ε is the lattice strain and the other parameters have the same

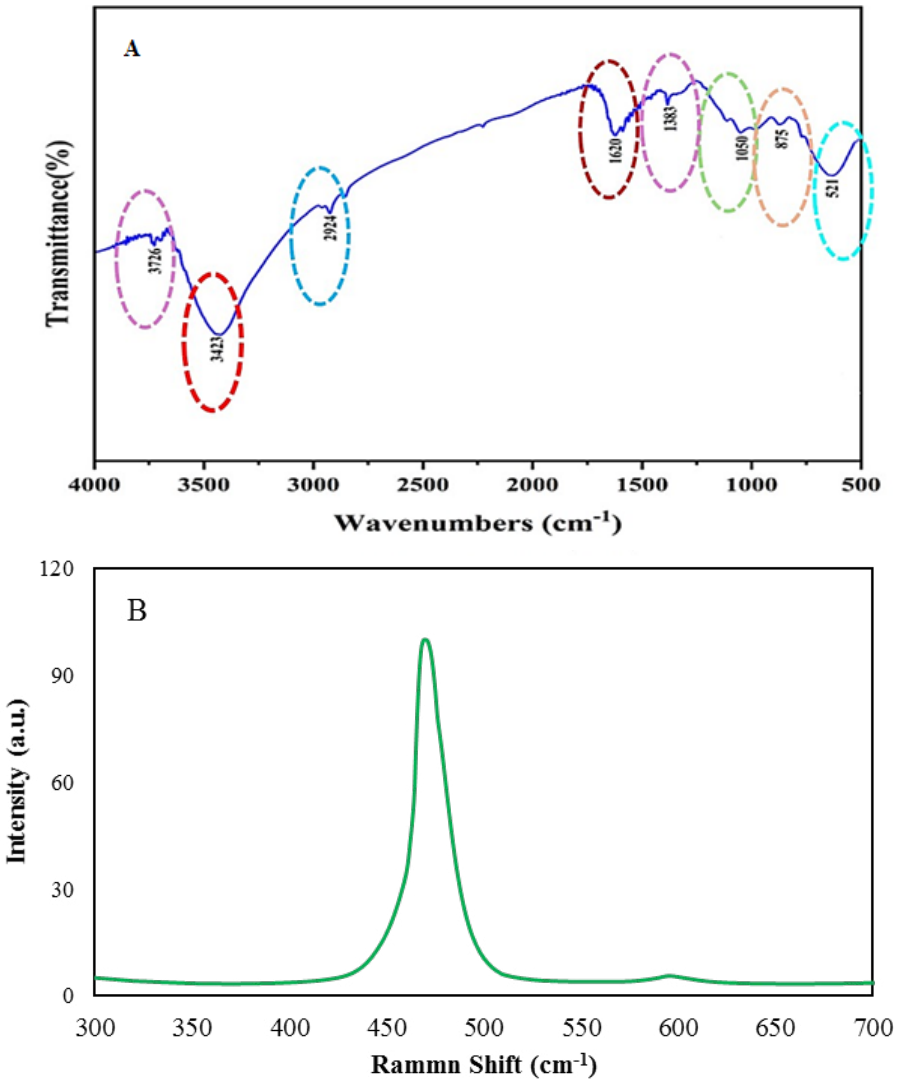

Fig. 1. (A) FT-IR and (B) Raman-scattering spectra of synthesized CeO_2 nanoparticles.

meanings as previously defined) considers both size-induced and strain-induced broadening of X-ray diffraction (XRD) peaks. In practice, A plot of βcosθ versus 4sinθ is drawn, and the lattice strain is obtained from the slope, while the crystallite size (D) is determined from the y-intercept. The estimated average crystallite size was found to be 9.8 nm, which is in good agreement with the value obtained from the Scherrer equation. The lattice strain was calculated to be 3.6×10^{-4} indicating a minimal distortion in the crystal lattice.

XRD analysis confirmed the successful synthesis of phase-pure cerium oxide nanoparticles. The crystallite size analysis indicates particle dimensions in the nanometer range, while the lattice parameter calculations reveal a slight contraction compared to bulk material. These structural characteristics are typical of CeO_2 nanoparticles and confirm their potential for various technological applications requiring high surface area and unique catalytic properties.

The UV-Vis absorption spectrum of cerium oxide nanoparticles exhibits a characteristic absorption peak at λ_{max} = 358 nm (Fig. 3). This absorption band corresponds to electronic transitions between Ce^{3+} and Ce^{4+} oxidation states, indicating the presence of mixed valence states in the CeO_2 nanostructure. This observation is consistent with the expected optical behavior of nanosized CeO_2 and supports the successful formation of the intended nanostructure. The observed absorption maximum is attributed to charge transfer transitions within the cerium oxide lattice and serves as a distinctive spectroscopic signature for

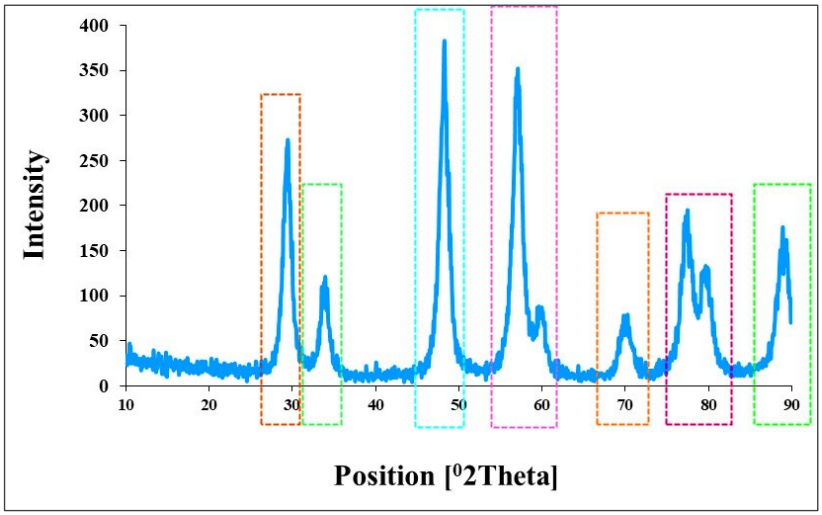

Fig. 2. XRD patterns of prepared CeO_2 nanoparticles.

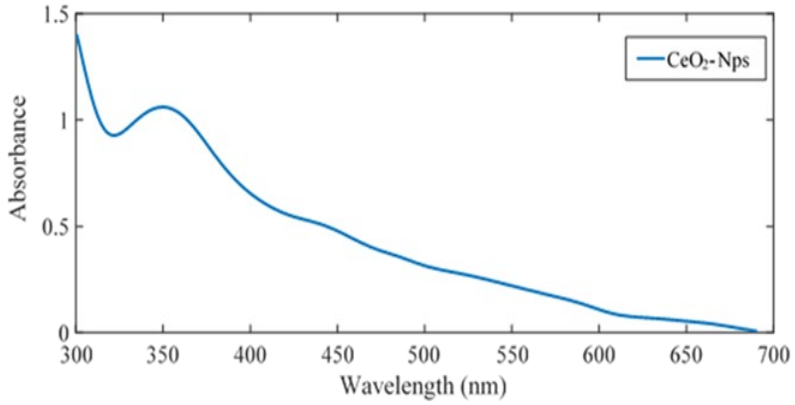

Fig. 3. Uv-Vis spectra of CeO_2 nanoparticles.

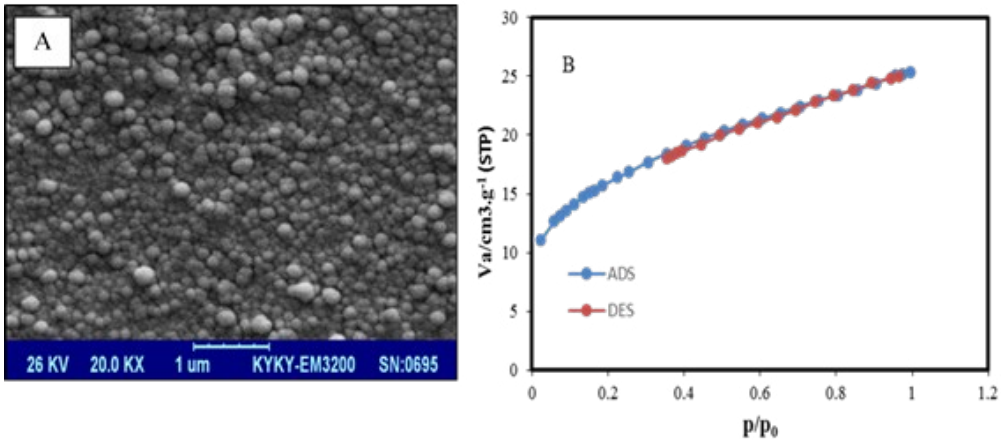

Fig. 4. (A) The SEM images (B) Nitrogen adsorption–desorption isotherms for synthesized CeO_2 nanoparticles.

CeO_2 nanoparticles [50]. The clarity and position of this peak further reinforce the uniformity and stability of the synthesized nanoparticles.

SEM images of the synthesized cerium oxide (CeO_2) nanoparticles reveal predominantly spherical morphology with well-defined particle boundaries (Fig. 4A). Analysis of SEM micrographs demonstrates that the nanoparticles possess a relatively narrow size distribution within the nanoscale range. Based on the obtained results from the SEM images, the average particle size is approximately ~10-12 nm, confirming their nanoscale dimensions. The spherical geometry and consistent particle dimensions suggest optimal synthesis conditions were maintained throughout the preparation process. This uniformity in both shape and size indicates that the growth process proceeded in a controlled manner and that the synthesis parameters were effectively controlled. Fig. 4B shows the nitrogen adsorption–desorption isotherms for synthesized CeO_2 nanoparticles. The BET analysis of the synthesized cerium oxide (CeO_2) nanoparticles revealed a specific surface area of 57.58 m^2/g, indicating a high surface tovolume ratio typical of nanoscale materials. Such a large surface area is beneficial for applications involving catalysis, adsorption, or sensor technologies, as it provides more active sites for reactions or interactions. The average pore diameter was found to be approximately 2.71 nm. Together, these BET results demonstrate that the synthesized CeO_2 nanoparticles have a favorable textural property profile and high surface area which can enhance their performance in catalytic processes. To obtain a more detailed description of the pore structure, the adsorption data were further analyzed using the non-linear density functional theory (NLDFT) model. The NLDFT surface area was found to be slightly higher than the BET value (~59.1 m^2/g), which is expected due to the higher sensitivity of NLDFT to subtle surface irregularities and interparticle voids. The pore diameter distribution was found to be ~3 nm. Both methods report similar values for the porosity and surface area of the nanoparticles. However, a slight discrepancy between them arises because the NLDFT method is more sensitive to fine structural details; due to its ability to account for surface roughness and small interparticle cavities, it reports a slightly higher surface area.

3.2 study on the surface of electrode

An approximate estimate for the active surface area of the electrode was carried out using the Randles–Sevcik equation [51].

$$I_{peak} = 2.69 \times 10^5 \, n^{3/2} A D^{1/2} C \upsilon^{1/2} \quad (1)$$

Where I_{peak} is the anodic peak current, A is the surface area (cm^2), υ is the scan rate ($mV.s^{-1}$), n=1, D is the diffusion coefficient (7.6×10^{-6} cm^2/s), and the other symbols have their usual meanings. Using Randles–Sevcik equation and the slope of I_{peak} versus $\upsilon^{1/2}$ in a 1.0 mM $K_4[Fe(CN)_6]^{3-/4-}$ solution, microscopic areas for CPE and CeO_2/CPE were calculated to be 0.061, 0.1201 cm^2, respectively. The active surface area confirms that modifying the electrode surface with CeO_2 causes an enhancement of surface area and an increase in the oxidation current of Dop.

Electrochemical impedance spectroscopy (EIS) was employed to investigate the modification of

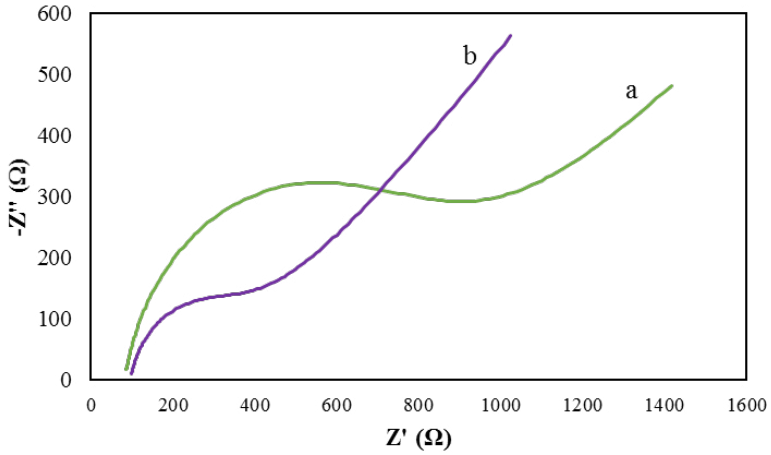

Fig. 5. Nyquist plot of (a) CPE and (b) CeO_2/CPE at the solution containing 1.0 mM $[Fe(CN)_6]^{3-/4-}$.

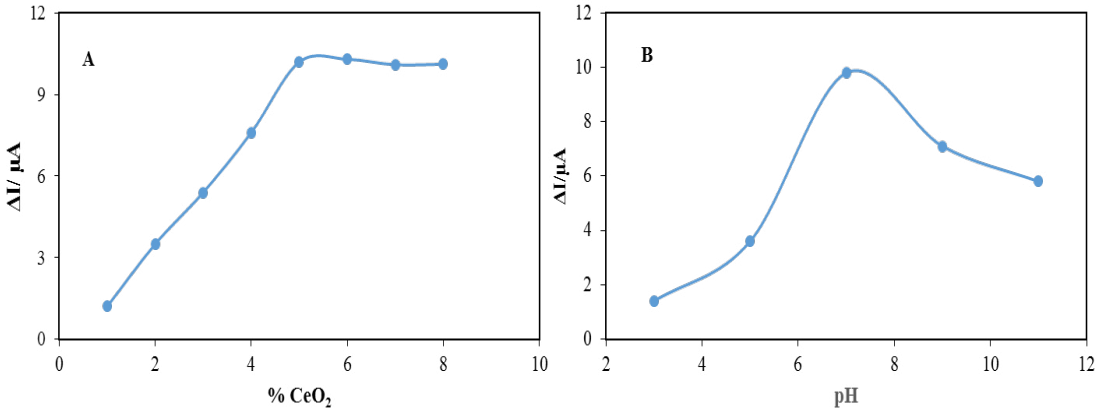

Fig. 6. Optimization of operating conditions: (A) the percentages of CeO_2 in CPE, (B) Variation of anodic peak current of CeO_2 vs. pH in the presence of dopamine (0.5mM) in Phosphate buffer solution.

the surface CPE with CeO_2 nanoparticles. One of the most common formats for interpreting EIS data is the Nyquist plot, which consists of a semicircle followed by a straight line. A semicircle is related to the charge-transfer process, whereas the line region corresponds to the diffusion-controlled process. The diameter of the semicircle is proportional to the electron transfer resistance (R_{ct}) of the working electrode, whereas the Warburg line indicates the mass transfer. The Nyquist plots of the CPE and CeO_2/CPE in 1.0 mM $[Fe(CN)_6]^{3-/4-}$ were shown in Figure 5. Based on the results shown in Figure 5, when the CPE was modified with CeO_2 (Fig. 5 curve b), the diameter of the semicircle portion (R_{ct}) decreased compared with that of the CPE (Fig. 5 curve a), and the surface area was improved. Therefore, R_{ct} was lower than that of unmodified CPE due to the high conductivity and large surface area of CeO_2 nanoparticles. The reduction of resistance in the CeO_2/CPE electrode, due to the properties of the cerium oxide nanoparticles, enhances the efficiency of this electrode in determination of dopamine.

3.3 The optimization of experimental parameters

To increase the sensitivity of the electrochemical CeO_2/CPE sensor, the experimental parameters, including the CeO_2 nanoparticles percentage and the solution pH, were optimized. The influence of CeO_2 present in the structure of carbon paste on the oxidation peak current of dopamine was studied in the range of 1.0 to 8 % w/w and the scan rate of 30 $mV.s^{-1}$. The results indicated that the changes of peak currents (ΔI) are increased by increasing

the percentages of CeO_2 in the structure of carbon paste, up to 5.0 % w/w and then by increasing the percentage of CeO_2, the values of ΔI will be constant therefore, 5.0 % w/w of CeO_2 was selected as the optimum percentage of CeO_2 (Fig. 6A). The oxidation of dopamine shows a strong dependence to pH. According to Fig. 6B, the values of oxidation peak currents are increased by increasing the pH up to 7, and then the value of the peak current will be decreased. So, the optimum value of pH was selected as 7, and other experiments were performed under this pH.

3.4 Investigation of the electrooxidation of dopamine at CeO_2/CPE sensor

Fig. 7 indicates the cyclic voltametric responses of different electrodes in the absence and presence of 0.5 mM dopamine as follows: CPE (curve a), CeO_2/CPE (curve b) in the absence of dopamine, and CPE (curve c), CeO_2/CPE (Curve d) in the presence of dopamine, respectively. Based on the results obtained from this figure, the carbon paste electrodes and carbon paste electrodes modified with cerium oxide nanoparticles showed no oxidation and reduction peaks in phosphate buffer solution with pH=7 (Fig. 7, curves a and b). When the carbon paste electrode was placed in a solution containing dopamine, the oxidation and reduction peaks related to this compound were observed at a potential of approximately 0.28 V (Fig. 7 curve c). When the carbon paste electrode modified with cerium oxide nanoparticles was placed in this solution, the current related to the oxidation of this compound increased and its potential decreased (Fig. 7 curve d). The results obtained from cyclic voltammetry showed that the carbon paste electrode modified with cerium oxide nanoparticles acts as a suitable platform for the oxidation and measurement of dopamine. According to the obtained results, from curve d in fig. 7 the anodic peak current of dopamine at CeO_2/CPE is increased and its cathodic peak is omitted on the reverse scan of the potential. The above observations indicated that an electrocatalytic mechanism is seen for oxidation of dopamine at the surface of CeO_2/CPE sensor.

3.5 Differential pulse voltammetry investigation

The differential pulse voltammograms (DPVs) were achieved for various concentrations of dopamine in Phosphate buffer solution (pH=7.0). The result is exhibited in Fig. 8. The dopamine electrocatalytic peak current at the surface of the CeO_2/CPE sensor can be attributed to the dopamine concentration. According to the calibration curve, the linear range was obtained from 0.5- 80 μM (inset Fig. 8). Also, the detection limit according to ($3s_b/m$) for oxidation of dopamine was determined to be 0.17 μM. Comparison of the efficiency of fabricated sensor with other methods for determination of dopamine was carried out and the results are summarized in Table 1. Based on the results presented in this table, it can be observed that the sensor developed in this work exhibits a suitable limit of detection (LOD) and linear range compared to other studies.

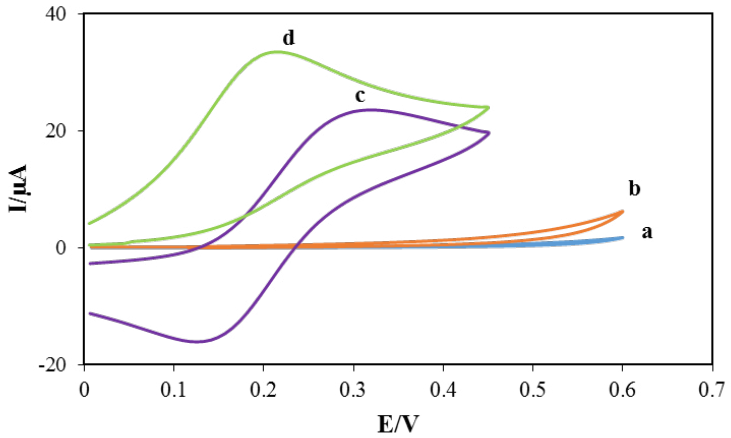

Fig. 7. CVs obtained at (a) CPE, (b) CeO_2/CPE in the absence of dopamine, (c) CPE, (d) CeO_2/CPE in a 0.50 mM dopamine solution at a scan rate of 30 mVs^{-1}.

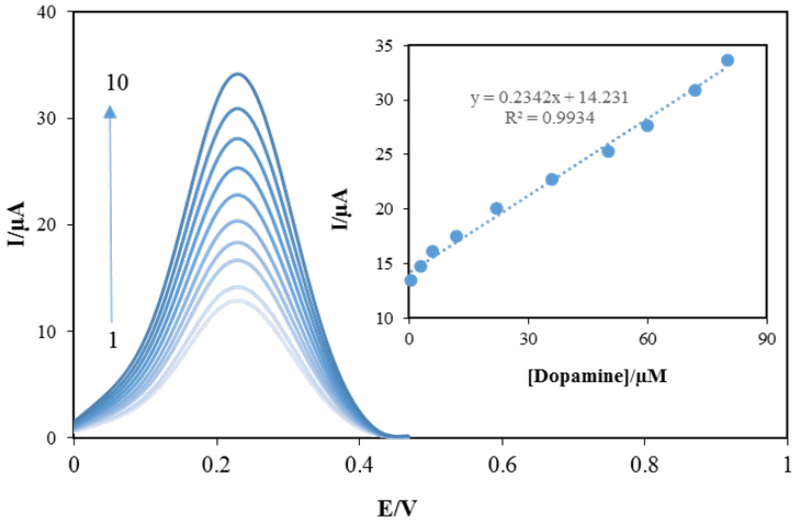

Fig. 8. DPVs of CeO2/CPE in Phosphate buffer solution (pH=7.0) contain different concentrations of dopamine (numbers 1-10correspond to 0.5 to 80.0 µM of dopamine). Insects: The plots of the electrocatalytic peak current as a function of dopamine concentration in the range of 0.5 to 80.0 µM.

Table 1. Comparison of the proposed method with some reported methods for determination of dopamine.

Modification Materials	Method	LOD (µM)	LDR (µM)	Ref.
GO/Fe_3O_4	CV and DPV	0.48	1.0-10.0	[52]
SPCE/TiO_2NP/AuNP/PNBDES	DPV	0.068	0.075-62.5	[53]
Co_3O_4/CuO/SDS	CV	0.6	1.0-80.0	[54]
SnO_2/chitosan	DPV and CV	0.77	1.0-18.0	[55]
CeO_2/ CPE	DPV	0.17	0.50-80.0	Present study

3.6 Selectivity, reproducibility, and stability of CeO_2/CPE sensor

Analytical selectivity constitutes a critical parameter in electrochemical sensor characterization, as it directly governs the reliability and specificity of the developed sensing platform. To evaluate the anti-interference capability of the fabricated sensor, a comprehensive selectivity study was conducted by examining the electrochemical response of dopamine (0.5 mM) in the presence of potential interfering species, including acetaminophen, glucose, adrenaline, uric acid, diclofenac, dexamethasone, paroxetine, epinephrine and estradiol (each at 0.1 mM concentration).

According to the obtained results in Table 2, the electrochemical measures demonstrated that the anodic peak current intensity of dopamine remained unperturbed despite a 10-fold excess (and even in some cases, with a higher ratio (concentration of the interfering species. The study is that if the current from the presence of the interfering species is less than 5 % different from the peak current of the dopamine in the absence of the interferences, such interference will not interfere with the measurement of the dopamine. These findings substantiate the exceptional selectivity coefficient of the CeO_2/CPE-modified electrode, confirming its capability to discriminate dopamine from structurally similar compounds and common biological interfering species with high specificity and minimal cross-reactivity. The analytical reproducibility of the CeO_2/CPE sensor was systematically evaluated through inter-electrode precision studies. Five independent CeO_2/CPE electrodes were fabricated following identical preparation protocols, and their electrochemical performance was assessed via differential pulse voltammetry (DPV) for dopamine quantification at a fixed concentration of 50 µM. Statistical analysis of the voltammetric responses yielded a relative standard deviation (RSD) of 3.8%, demonstrating satisfactory inter-electrode reproducibility and consistent fabrication methodology. This low RSD

Table 2. The influence of interfering species on the measurement of 0.5 mM Dopamine using the CeO_2/CPE electrode (pH= 8).

Species	The concentration ratio of interferences species to DO	Signal change (%)
Acetaminophen	10	0.35
Glucose	10	0.42
Adrenaline	10	0.48
Uric acid	12	1.11
Diclofenac	10	0.89
Dexamethasone	5	1.23
Paroxetine	10	0.75
Epinephrine	12	1.96
Estradiol	5	2.11

Table 3. Determination of dopamine in real samples using the designed sensor (pH=7, n=5).

Sample number	Added (µM)	RSD%	Measured by sensor (µM)	Recovery%
1	20	1.11	19.35	96.75
2	30	1.24	29.21	97.63

value confirms the reliability and precision of the sensor fabrication process, indicating minimal batch-to-batch variation and excellent analytical repeatability for dopamine detection. The temporal stability and operational longevity of the CeO_2/CPE electrochemical sensor were systematically investigated through chronological performance monitoring under ambient laboratory conditions. The fabricated sensor was subjected to accelerated aging studies at room temperature with periodic electrochemical evaluation at predetermined time intervals. Differential pulse voltammetric measurements for dopamine electro-oxidation were conducted at 4-day, 1-week, and 2-week intervals to assess signal retention and electrode degradation kinetics. The anodic peak current responses demonstrated exceptional temporal stability, retaining 97.3%, 96.6%, and 96.1% of the initial electrochemical activity after 4 days, 7 days, and 14 days of storage, respectively.

The minimal signal attenuation indicates superior electrode stability with negligible active surface deterioration and maintained electrocatalytic efficiency. This remarkable temporal performance validates the structural integrity and operational robustness of the CeO_2/CPE sensing platform, confirming its suitability for prolonged analytical applications with consistent electrochemical response characteristics.

3.7 Determination of dopamine in real samples

The applicability of the CeO_2/CPE sensor was investigated by the determination of dopamine in the real samples (pH=7). The fabricated sensor was applied to two blood serum samples obtained from a local hospital. Prior to the determination of dopamine in blood serum samples, since blood serum contains high concentrations of proteins that can bind the drug and interfere with measurement, a protein precipitation step is performed, commonly by adding organic solvent such as acetonitrile or methanol in a typical ratio of 1:3 (serum: solvent). The mixture is vortexed and centrifuged again to pellet the proteins, leaving a clear supernatant containing the serum. In some workflows, additional filtration may be applied to remove residual particulates or lipids and further minimize matrix effects. The prepared serum supernatant can then be directly used for analysis. These pretreatment steps serum separation, protein removal, and optional clarification are essential to ensure accurate, reproducible, and reliable quantification of the drug. Then, dopamine solutions with specific concentrations were added to the diluted serum solutions. The quantitative determination of dopamine in blood serum samples was performed, and the recovery percentages are obtained (Table 3). Based on the obtained results from recovery percentages, it can

be concluded that the designed sensor is applicable for the determination of dopamine in blood serum samples.

4. Conclusion

In the present study, a new carbon paste electrode modified with CeO_2 as an electrochemical sensor was constructed to determine Dop. The synthesized cerium oxide nanoparticles were characterized using Fourier-transform infrared spectroscopy (FTIR), X-ray diffraction analysis (XRD), scanning electron microscopy (SEM), Raman and UV-visible spectroscopy (UV-Vis).

Based on the obtained results from various characterizations, the synthesis of cerium oxide nanoparticles was successfully achieved, and these nanoparticles were used to modify the carbon paste electrode (CeO_2/CPE). The electrochemical oxidation and determination of dopamine was studied by cyclic voltammetry and differential pulse voltammetry with proposed electrode. The capability of this sensor to be used in real samples makes it a proper platform for the Dop determination in biological fluids such as human blood serum samples. This electrochemical sensor can enhance electrical conductivity even at low concentrations, and its high sensitivity and stability, good selectivity, simplicity of fabrication, lower detection limit, and wide linear range make it superior to previously reported methods.

Acknowledgements

The authors wish to thank Vali-e-Asr University of Rafsanjan Research Council for the financial support of this research.

References

[1] S.B. Matt, S. Manjunatha, S. Manjunatha, D. M. Sidlingappa, M. Sidlingappa, Synthesis of Cerium-Doped Zirconia Nanoparticles for the Electrochemical Detection of Dopamine by Modified Carbon Paste Electrode, Chemistry Select. 4 (2019) 5839-5844. https://doi.org/10.1002/slct.201900642

[2] S. A Zaidi, Development of molecular imprinted polymers based strategies for the determination of Dopamine, Sens. Actuators B: Chem. 265 (2018) 488-497. https://doi.org/10.1016/j.snb.2018.03.076

[3] R. Afsharipour, S. Dadfarnia, A. M. Haji Shabani, Chemiluminescence determination of dopamine using N, P-graphene quantum dots after preconcentration on magnetic oxidized nanocellulose modified with graphene quantum dots, Microchim. Acta, 192 (2022) 1-12. https://doi.org/10.1007/s00604-022-05251-3

[4] M. Chen, Y. Meng, W. Zhang, J. Zhou, J. Xie, G. Diao, β-Cyclodextrin polymer functionalized reduced-graphene oxide: Application for electrochemical determination imidacloprid Electrochim. Acta, 108 (2013) 1-9. https://doi.org/10.1016/j.electacta.2013.06.050

[5] Y. Oztekin, M. Tok, E. Bilici, L. Mikoliunaite, Z. Yazicigil, A. Ramanaviciene, A. Ramanavicius,Copper nanoparticle modified carbon electrode for determination of dopamine, Electrochim. Acta, 76(2012) 201-207. https://doi.org/10.1016/j.electacta.2012.04.105

[6] X. Zhang, Y. C. Zhang, L. X. Ma, 2016, One-pot facile fabrication of graphene-zinc oxide composite and its enhanced sensitivity for simultaneous electrochemical detection of ascorbic acid, dopamine and uric acid, Sens. Actuators B: Chem., 227(2016) 488-496. https://doi.org/10.1016/j.snb.2015.12.073

[7] D. B. Gorle, M. A. Kulandainathan, Electrochemical sensing of dopamine at the surface of a dopamine grafted graphene oxide/poly(methylene blue) composite modified electrode RSC Adv., 6 (2016) 19982-19991. https://doi.org/10.1039/C5RA25541D

[8] H. Xiong, B. Jin, The electrochemical behavior of AA and DA on graphene oxide modified electrodes containing various content of oxygen functional groups J. Electroanal. Chem., 661 (2011) 77-83. https://doi.org/10.1016/j.jelechem.2011.06.034

[9] D. Kim, S. Lee, Y. Piao, Electrochemical determination of dopamine and acetaminophen using activated graphene-Nafion modified glassy carbon electrode, J. Electroanal. Chem., 794 (2017) 221-228. https://doi.org/10.1016/j.jelechem.2017.04.018

[10] C. Xue, Q. Han, Y. Wang, J. Wu, T. Wen, R. Wang, J. Hong, X. Zhou, H. Jiang, Amperometric detection of dopamine in human serumby electrochemical sensor based on gold nanoparticles doped molecularly imprinted polymers Biosens. Bioelectron., 49 (2013) 199-203. https://doi.org/10.1016/j.bios.2013.04.022

[11] Y. Ogawa, S. Tsugita, Y. Torii, H. Iwamoto, T. Sato, J. Kasahara, M. Takeuchi, Microdialysis-integrated HPLC system with dual-electrode detection using track-etched membrane electrodes for in vivo monitoring of dopamine dynamics, J. Chromatogr. B, 1247 (2024) 124318. https://doi.org/10.1016/j.jchromb.2024.124318

[12] M. Shivakumar, K. L. Nagashree, S. Manjappa, M. S. Dharmaprakash, Electrochemical detection of nitrite using glassy carbon electrode modified with silver nanospheres (AgNS) obtained by green synthesis using pre-hydrolysed liquor, Electroanalysis, 29 (2017) 1434-1442. https://doi.org/10.1002/elan.201600775

[13] H. Moradpour, H. Beitollahi, Simultaneous electrochemical sensing of dopamine, ascorbic acid, and uric acid using nitrogen-doped graphene sheet-modified glassy carbon electrode, C, 8 (2022) 50. https://doi.org/10.3390/c8040050

[14] R. Monsef, M. Salavati-Niasari, Hydrothermal architecture of Cu5V2O10 nanostructures as new electro-sensing catalysts for voltammetric quantification of mefenamic acid in pharmaceuticals and biological samples, Biosens. Bioelectron., 178 (2021) 1-9. https://doi.org/10.1016/j.bios.2021.113017

[15] R. Monsef, M. Salavati-Niasari, Electrochemical sensor based on a chitosan-molybdenum vanadate nanocomposite for detection of hydroxychloroquine in biological samples, J. Colloid Interface Sci., 613 (2022) 1–14. https://doi.org/10.1016/j.jcis.2022.01.012

[16] N. Soltani, M. Khayatkashani, J. Ebrahimian, N. Tavakkoli, A. Rezaei, A. Ryadh, M. Salavati-Niasari, A novel modified CPE using CE-ZnO-Lapis lazuli nanocomposite as a sensitive electrochemical sensor for the determination of anti-cancer drug of etoposide, J. Alloys Compd., 968 (2023) 171900. https://doi.org/10.1016/j.jallcom.2023.171900

[17] H. Mahmoudi-Moghaddam, M. Amiri, H. Akbari Javar, Q.A. Yousif, M. Salavati-Niasari, Green synthesis and characterization of Tb-Fe-O-Cu ceramic nanocomposite and its application in simultaneous electrochemical sensing of zinc, cadmium and lead, Arab. J. Chem., 15 (2022) 103988. https://doi.org/10.1016/j.arabjc.2022.103988

[18] M. Goudarzi, M. Salavati-Niasari, M. Motaghedifard, S.M. Hosseinpour-Mashkani, Semiconductive Tl_2O_3 nanoparticles: facile synthesis in liquid phase, characterization and its applications as photocatalytic substrate and electrochemical sensor, J. Mol. Liq., 219 (2016) 720–727. https://doi.org/10.1016/j.molliq.2016.04.054

[19] H. Mahmoudi-Moghaddam, M. Amiri, H. Akbari Javar, Q.A. Yousif, M. Salavati-Niasari, A facile green synthesis of a perovskite-type nanocomposite using Crataegus and walnut leaf for electrochemical determination of morphine, Anal. Chim. Acta, 1203 (2022) 339691. https://doi.org/10.1016/j.aca.2022.339691

[20] M. Baladi, M. Amiri, H. Akbari Javar, H. Mahmoudi-Moghaddam, M. Salavati-Niasari, Green synthesis of perovskite-type TbFeO3/CuO as a highly efficient modifier for electrochemical detection of methyldopa, J. Electroanal. Chem., 915 (2022) 116339. https://doi.org/10.1016/j.jelechem.2022.116339

[21] J. Ebrahimian, M. Khayatkashani, N. Soltani, H.T. Mohammed, N. Tavakkoli, M. Jafari, M. Salavati-Niasari, Rosa Damascena mediated ZnO-Red Ochre nanocomposite for the electrochemical determination of 5-Fluorouracil, Arab. J. Chem., 16 (2023) 104586. https://doi.org/10.1016/j.arabjc.2023.104586

[22] P. Gai, H. Zhang, Y. Zhang, W. Liu, G. Zhu, X. Zhang, Simultaneous electrochemical detection of ascorbic acid, dopamine and uric acid based on nitrogen doped porous carbon nanopolyhedra, J. Chen, J. Mater. Chem. B, 1 (2013) 2742-2749. https://doi.org/10.1039/C3TB20215A

[23] Y. Li, M. Yao, T.-T. Li, Y.-Y. Song, Y.-J. Zhang, S.-Q. Liu, Simultaneous electrochemical determination of uric acid and dopamine in the presence of ascorbic acid using nitrogen-doped carbon hollow spheres, Anal. Methods, 5(2013) 3635-3638. https://doi.org/10.1039/C3AY40565F

[24] C. L. Sun, C. T. Chang, H. H. Lee, J. Zhou, J. Wang, T. K. Sham, W. F. Pong, Microwave-assisted synthesis of a core–shell MWCNT/GONR heterostructure for the electrochemical detection of ascorbic acid, dopamine, and uric acidACS Nano, 5 (2011) 7788-7795. https://doi.org/10.1021/nn2015908

[25] Y. Fan, H. Lu, J. Liu, C. Yang, Q. Jing, Y. Zhang & X. Yang, Hydrothermal preparation and electrochemical sensing properties of TiO2–graphene nanocomposite, Colloids Surf. B, 83 (2011) 78-82. https://doi.org/10.1016/j.colsurfb.2010.10.048

[26] S. Paramparambath, S. Shafath, M. R. Maurya, J.J. Cabibihan, A. Al-Ali, R. A. Malik, K. K. Sadasivuni, Nonenzymatic electrochemical sensor based on CuO–MgO composite for dopamine detection, IEEE Sens. J., 21 (2021) 25597–25605. https://doi.org/10.1007/s00604-021-05142-z

[27] Y. Kumar, S. Pramanik, D. P. Das, Lanthanum ortho-ferrite ($LaFeO_3$) nano-particles based electrochemical sensor for the detection of dopamine, Biointerface Res. Appl. Chem., 10 (2020) 6182–6188. https://doi.org/10.33263/BRIAC105.61826188

[28] S. E. Elugoke, O. E. Fayemi, A. S. Adekunle, B. B. Mamba, T. T. I. Nkambule, E. E. Ebenso, Electrochemical sensor for the detection of dopamine using carbon quantum dots/copper oxide nanocomposite modified electrode, Flat Ch., 33 (2022) 100372. https://doi.org/10.1016/j.flatc.2022.100372

[29] M. I. Khan, N. Muhammad, M. Tariq, U. Nishan, A. Razaq, T. A. Saleh, M. Abu Haija, I. Ismail, A. Rahim, Non-enzymatic electrochemical dopamine sensing probe based on hexagonal shape zinc-doped cobalt oxide ($Zn–Co_2O_4$) nanostructure, Microchim. Acta, 189 (2022) 37. https://doi.org/10.1007/s00604-021-05142-z

[30] M. Valian, A. Khoobi, M. Salavati-Niasari, Synthesis, characterization and electrochemical sensors application of $Tb_2Ti_2O_7$ nanoparticle modified carbon paste electrode for the sensing of mefenamic acid drug in biological samples and pharmaceutical industry wastewater, Talanta, 247 (2022) 123593. https://doi.org/10.1016/j.talanta.2022.123593

[31] M. Amiri, M. Salavati-Niasari, A. Akbari, A magnetic $CoFe_2O_4/SiO_2$ nanocomposite fabricated by the sol-gel method for electrocatalytic oxidation and determination of L-cysteine, Microchim. Acta, 184 (2017) 825–833. https://doi.org/10.1007/s00604-016-2064-4

[32] H. Madanakumara, H. S. Jayanna, C. V. Yelamaggad, S. Soundeswaran, M. Vishwas, K. S. Shamala, B. S. Surendra, N. Basavaraju, Enhanced electrochemical sensor and photodegradation of industrial wastewater by Almond gum assisted synthesis of Bi_2O_3/MgO/Fe_2O_3 nanocomposites, Sens. Int., 3 (2022) 100193. https://doi.org/10.1016/j.sintl.2022.100193

[33] H. Gao, J. Chai, C. Jin, M. Tian, Molecularly imprinted electrochemical sensor based on CoNi-MOF/RGO nanocomposites for sensitive detection of hippuric acid, Anal. Chim. Acta, 1296 (2024) 342307. https://doi.org/10.1016/j.aca.2024.342307

[34] F. Li, L. Liu, T. Liu, M. Zhang, Ni-MOF nanocomposites decorated by Au nanoparticles: an electrochemical sensor for detection of uric acid, Ionics, 28 (2022) 4843–4851. https://doi.org/10.1007/s11581-022-04712-2

[35] J. Zheng, J. Xiao, J. G. Zhang, The roles of oxygen non-stoichiometry on the electrochemical properties of oxide-based cathode materials, Nano Today, 11 (2016) 678-694. https://doi.org/10.1016/j.nantod.2016.08.011

[36] L. Renuka, K. S. Anantharaju, S. C. Sharma, H. P. Nagaswarupa, S. C. Prashantha, H. Nagabhushana, Y. S. Vidya, Hollow microspheres Mg-doped ZrO2 nanoparticles: green assisted synthesis and applications in photocatalysis and photoluminescence, J. Alloys Compd., 672 (2016) 609-622. https://doi.org/10.1016/j.jallcom.2016.02.124

[37] S. Saeednia, M. Rezaeinasab, P. Iranmanesh, S. A. Razgaleh, A metal organic framework, UiO-66-NH 2, based on a molybdenum Schiff base complex for the efficient electrochemical determination of diphenoxylate Anal. Methods, 17 (2025) 762-771. https://doi.org/10.1039/D4AY01957A

[38] D. R. Miller, S. A. Akbar, P. A. Morris, Nanoscale metal

oxide-based heterojunctions for gas sensing: A review, Sens. Actuators B: Chem., 204 (2014) 250-272. https://doi.org/10.1016/j.snb.2014.07.074

[39] Y. Wei, Q. A. Huang, M. G. Li, X. J. Huang, B. Fang, L. Wang, CeO_2 nanoparticles decorated multi-walled carbon nanotubes for electrochemical determination of guanine and adenine, Electrochim. Acta, 56 (2011) 8571-8575. https://doi.org/10.1016/j.electacta.2011.07.048

[40] Y. Temerk, H. Ibrahim, A new sensor based on In doped CeO_2 nanoparticles modified glassy carbon paste electrode for sensitive determination of uric acid in biological fluids, Sens. Actuators B: Chem., 224 (2016) 868-877. https://doi.org/10.1016/j.snb.2015.11.029

[41] P. Tamizhdurai, S. Sakthinathan, S. M. Chen, K. Shanthi, S. Sivasanker, P. Sangeetha, Environmentally friendly synthesis of CeO_2 nanoparticles for the catalytic oxidation of benzyl alcohol to benzaldehyde and selective detection of nitrite, Sci. Rep., 7 (2017) 1-13. https://doi.org/10.1038/srep46372

[42] C. Walkey, S. Das, S. Seal, J. Erlichman, K. Heckman, L. Ghibelli, E. Traversa, J. F. McGinnis, W. T. Self, Catalytic properties and biomedical applications of cerium oxide nanoparticles, Environ. Sci.: Nano, 2 (2015) 33-53. https://doi.org/10.1039/C4EN00138A

[43] N. Selvakumar, K. Jeyasubramanian, R. Sharmila, Smart coating for corrosion protection by adopting nano particles, Prog. Org. Coat., 74 (2012) 461-469. https://doi.org/10.1016/j.porgcoat.2012.01.011

[44] M. K. Fauzia, M. Chaman, A. Azam, Antibacterial and sunlight-driven photocatalytic activity of graphene oxide conjugated CeO_2 nanoparticles, Sci. Rep., 14 (2024) 6606. https://doi.org/10.1038/s41598-024-54905-0

[45] A. Q. Wang, N. D. Souza, T. D. Golden, Electrosynthesis of nanocrystalline cerium oxide/layered silicate powders, J. Mater. Chem., 16 (2006) 481-488. https://doi.org/10.1039/B506976A

[46] J. Farhangi, M. A. Es-Haghi, M. E. Taghavizadeh Yazdi, A. Rahdar, F. Baino, MOF-mediated synthesis of CuO/CeO_2 composite nanoparticles: Characterization and estimation of the cellular toxicity against breast cancer cell line (MCF-7), J. Funct. Biomater., 12 (2021) 53. https://doi.org/10.3390/jfb12040053

[47] D. Kim, S. Townsley, V. H. Grassian, Vibrational spectroscopy as a probe of heterogeneities within geochemical thin films on macro, micro, and nanoscales, RSC Adv., 13 (2023) 28873–28884. https://doi.org/10.1039/D3RA05179J

[48] G. Wang, Q. Mu, T. Chen, Y. Wang, Synthesis, characterization and photoluminescence of CeO_2 nanoparticles by a facile method at room temperature, J. Alloys Compd., 493 (2010) 202–207. https://doi.org/10.1016/j.jallcom.2009.10.140

[49] A. Miri, M. Sarani, Biosynthesis, characterization and cytotoxic activity of CeO2 nanoparticles, Ceram. Int., 44 (2018) 12642-12647. https://doi.org/10.1016/j.ceramint.2018.04.063

[50] M. M. Ali, H. S. Mahdi, A. Parveen, and A. Azam, Optical properties of cerium oxide (CeO2) nanoparticles synthesized by hydroxide mediated method, AIP Conf. Proc., 1953 (2018) 030044. https://doi.org/10.1063/1.5032379

[51] M. Rezaeinasab, A. Benvidi, S. Gharaghani, H.R. Zare, Chemometrics approaches based on electrochemical methods for the investigation of interaction between bovine serum albumin and carvacrol with the aim of its application to protein sensing, J. Electroanal. Chem. 845 (2019) 48-56. https://doi.org/10.1016/j.jelechem.2019.05.040

[52] I. Anshori, K. A. Kepakisan, L. Nuraviana Rizalputri, R. Rona Althof, A. E. Nugroho, R. Siburian, M. Handayani, Facile synthesis of graphene oxide/Fe_3O_4 nanocomposite for electrochemical sensing on determination of dopamine, Nanocomposites, 8 (2022) 155–166. https://doi.org/10.3390/nanocomposites8010012

[53] A. Y. Kabaca, M. B. Kamac, M. Yılmaz, T. Atıcı, Ultra-sensitive electrochemical sensors for simultaneous determination of dopamine and serotonin based on titanium oxide-gold nanoparticles-poly Nile blue (in deep eutectic solvent), Electrochim. Acta, 467 (2023) 143046. https://doi.org/10.1016/j.electacta.2023.143046

[54] M. Kumar, B. E. Kumara Swamy, U. Chandra, A. W. Gebisa, Co_3O_4/CuO composite nanopowder/sodium dodecyl sulphate modified carbon paste electrode based voltammetric sensors for detection of dopamine, Int. J. Nanotechnol., 14 (2017) 930–944. https://doi.org/10.1504/IJNT.2017.085836

[55] S. Selvarajan, A. Suganthi, M. Rajarajan, A facile approach to synthesis of mesoporous SnO_2/chitosan nanocomposite modified electrode for simultaneous determination of ascorbic acid, dopamine and uric acid, Surf. Interfaces, 7 (2017) 146–156. https://doi.org/10.1016/j.surfin.2017.02.004